crystals

MDPI

Article

Concept Study for an Integrated Reactor-Crystallizer Process for the Continuous Biocatalytic Synthesis of (*S*)-1-(3-Methoxyphenyl)ethylamine

Dennis Hülsewede [1], Erik Temmel [2], Peter Kumm [1] and Jan von Langermann [1,*]

[1] Biocatalytic Synthesis Group, Institute of Chemistry, University of Rostock, Albert-Einstein-Str. 3A, 18059 Rostock, Germany; dennis.huelsewede@uni-rostock.de (D.H.); peter.kumm@uni-rostock.de (P.K.)
[2] Sulzer Chemtech Ltd., Gewerbestraße 28, 4123 Allschwil, Switzerland; temmel@mpi-magdeburg.mpg.de
* Correspondence: jan.langermann@uni-rostock.de; Tel.: +49-381-4986456

Received: 27 February 2020; Accepted: 23 April 2020; Published: 27 April 2020

Abstract: An integrated biocatalysis-crystallization concept was developed for the continuous amine transaminase-catalyzed synthesis of (*S*)-1-(3-methoxyphenyl)ethylamine, which is a valuable intermediate for the synthesis of rivastigmine, a highly potent drug for the treatment of early stage Alzheimer's disease. The three-part vessel system developed for this purpose consists of a membrane reactor for the continuous synthesis of the product amine, a saturator vessel for the continuous supply of the amine donor isopropylammonium and the precipitating reagent 3,3-diphenylpropionate and a crystallizer in which the product amine can continuously precipitate as (*S*)-1-(3-methoxyphenyl)ethylammonium-3,3-diphenylpropionate.

Keywords: amine; biocatalysis; enzyme; process intensification; crystallization; enantioselective

1. Introduction

In recent years, biocatalytic synthesis reactions have made a significant impact in the scientific community and have even replaced existing chemical pathways in industrial processes. The main advantages are often higher stereo-, regio- and chemoselectivities, while mild reaction conditions and environmentally friendly solvents such as water can be applied. The high selectivity of biocatalysts results also frequently in less or even no side reactions, which itself yields higher process and atom efficiencies. In addition, recent scientific and technological advances in enzyme engineering allow the relatively fast design and production of tailor-made biocatalysts for a specific process [1–7]. Furthermore, downstream-processing from biocatalyst-based reaction systems remains an issue and is a major economic factor in the overall process. This problem originates mostly from the presence of water-soluble proteins, buffer salts, biocatalyst-based cofactors, remaining unreacted substrates and co-substrates, which have to be removed efficiently to ensure high product purities. The purification from such complex mixtures is typically achieved by multiple extractions and further purification steps [8].

In contrast, selective crystallization techniques provide a more selective product isolation approach from complex mixtures, especially aqueous solutions and was integrated in this study directly into the biocatalytic synthesis process [9]. In the presented study this is utilized at the synthesis of (*S*)-1-(3-methoxyphenyl)ethylamine, which is a valuable intermediate for the synthesis of rivastigmine, a highly potent drug for the treatment of early stage Alzheimer's disease (Scheme 1). Studies have shown that the (*S*)-enantiomer is more potent as the (*R*)-enantiomer and preferably the enantiomerically pure (*S*)-form should be administered to avoid complications [10–13].

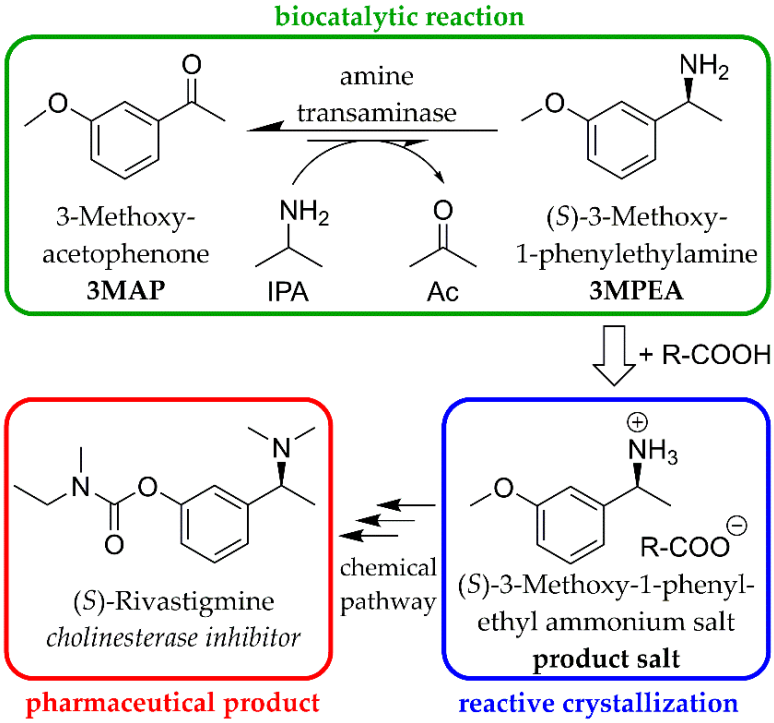

Scheme 1. Investigated biocatalytic transamination reaction and the inclusion of a reactive crystallization step for the synthesis of rivastigmine; R = $-CH_2-CHPh_2$.

The applied amine transaminase from *Ruegeria pomeroyi* catalyzes the transfer of the amine group from the donor amine isopropylamine (IPA) to the carbonyl compound 3-methoxyacetophenone (3MAP), forming (*S*)-1-(3-methoxyphenyl)ethylamine (3MPEA) and acetone (Ac) as a co-product [14,15]. The biocatalytic transformation forming 3MPEA itself is very enantioselective but suffers from an unfavorable reaction equilibrium [16]. These limitations in amine transaminase-catalyzed reactions are often overcome by classical (bio)chemical solutions to remove the co-product from the equilibrium or using specifically tailor-made donor amines to shift the reaction to the product side [17–28]. These chemically-driven options offer higher yields but require often a complex process control, additional (bio)catalytic reaction systems, additional chemicals and eventually lead to lower atom efficiencies [29]. As a crystallization-based alternative we apply our recently developed in situ-product crystallization approach in the amine-transaminase-catalyzed reaction [16,30]. This reactive crystallization approach removes the product amine 3MPEA from solution by forming an ammonium salt with a suitable carboxylate anion that exhibits a very low solubility. Additional chemical reactants or (bio)catalysts are not required and a simplified downstream-processing approach via filtration is possible.

2. Materials and Methods

2.1. Chemicals

All chemicals were obtained from Acros (Fair Lawn, NJ, USA), TCI Chemicals (Tokyo, Tokyo Prefecture, Japan), Aldrich (St. Louis, MO, USA), Alfa Aesar (Haverhill, MA, USA) and ABCR (Karlsruhe, Baden-Württemberg, Germany) and were used as received. Deionized water was used throughout this study.

2.2. Biocatalyst

Amine transaminase from *Ruegeria pomeroyi* (as ECS-ATA08) was obtained as whole cell lyophilizate (Enzymicals AG (Greifswald, Mecklenburg-Vorpommern, Germany)) and was used as received during this study. The activity of 364 U/g was determined using the conversion of 2.5 mmol/L 1-phenylethylamine and 2.5 mmol/L pyruvate to acetophenone and alanine in 50 mM phosphate buffer pH 8.0 with 0.025 mmol PLP and 0.25 %(v/v) DMSO at 25 °C. One unit of enzyme activity is defined as the formation of 1 mmol acetophenone per minute, which was observed spectrophotometrically at 245 nm with ε(acetophenone) = 11.852 L/(mol·cm).

2.3. Donor Amine Salt Synthesis

39.6 g 3,3-diphenylpropionic acid (3DPPA) were dissolved in 500 mL methyl tert-butyl ether (MTBE) in a 1 L round flask. Then 16.0 mL isopropylamine (IPA) were added to the stirred solution with a syringe and the resulting suspension was stirred overnight. MTBE and excess IPA were evaporated afterwards with a rotary evaporator to obtain the donor salt isopropylammonium 3,3-diphenylpropionate (IPA-3DPPA).

2.4. Solubility Measurements

Solubilities were measured in 10 mL 50 mM phosphate buffer with an excess of the respective solid salt to obtain a saturated solution. The resulting mixture was adjusted to the desired pH value and shaken for 7 days at 160 rpm and 30 °C. The pH was re-adjusted daily with NaOH and HCl, if required. The resulting mixture was then filtered to obtain a clear, saturated solution. For pH-dependent measurements a sample was diluted (typically 20×) for the absorption measurement of 3DPPA at 249 nm and compared with a calibration curve of 3DPPA in 50 mM phosphate buffer at the same pH (3DPPA concentration range: 3–0.5 mM, 1 cm cuvette path length). For temperature dependent solubility measurements, 25 mM 2-[4-(2-hydroxyethyl)piperazin-1-yl]ethanesulfonic acid buffer (HEPES) at pH 7.5 was used. After 7 days a 1 mL sample was taken, evaporated and the amount of salt determined gravimetrically with the subtraction of the amount of HEPES.

2.5. Reactor Setup

Two Plane flange vessels with a tempering jacket and a bottom drain valve of 250 mL (Pfaudler GmbH, Germany) were used as crystallizer and saturator. The membrane reactor consists of two Teflon chambers separated by a polyvinylidene fluoride transfer membrane (PVDF) with a cut-off of 0.2 µm (Bio-Rad Laboratories GmbH, Germany) (Figure 1). The vessels were connected with PharMed - BPT and Tygon LMT - 55 tubes (Saint - Gobain, France), tempered with the cooling bath thermostat Huber CC-K6 attached to a Pilot ONE control panel (both by Peter Huber Kältemaschinenbau AG, Germany) and stirred with overhead stirrers MICROSTAR 7.5 control. The membrane reactor was stirred with magnetic stirrers (IKA Werke, Germany). Two peristaltic pumps—Hei-FLOW Precision 01 (Heidolph Instruments, Germany)—were used to transfer the mother liquors from the saturator to the membrane reactor and from the crystallizer to the saturator. To ensure a constant filling level in the membrane reactor, an overflow was integrated from which the reaction solution can flow into the lower positioned crystallizer. In order to keep the solid salts in the saturator and the crystallizer, 11 µm filters have been placed at the inlet of the tubes.

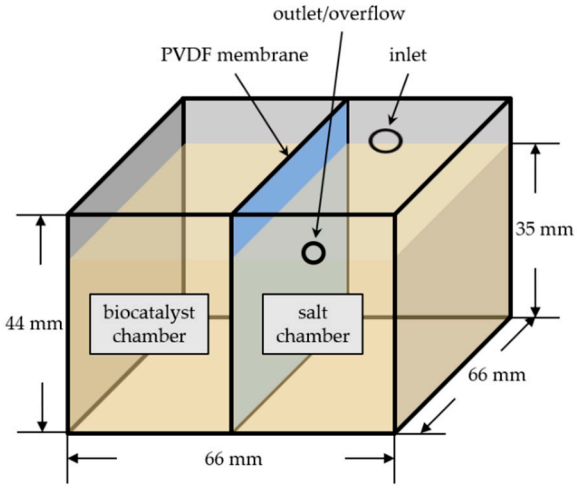

Figure 1. Design of the membrane reactor with polyvinylidene fluoride membrane (PVDF).

2.6. Membrane Reactor Procedure

In the membrane reactor, 857 µL IPA (100 mM) and 596 mg HEPES buffer (25 mM) were added to 100 mL water and the pH was adjusted to 7.5. This solution was divided equally into both chambers of the reactor. After the addition of 2.85 g donor salt (100 mM) and 566 mg product salt (26 mg for saturation and 540 mg as seed crystals) to the salt chamber, the reactor was stirred until the dissolved salts were homogeneously distributed in both chambers. To start the reaction, 124 mg pyridoxal 5′-phosphate (PLP) (5 mM) and 1.37 mL substrate 3′-methoxyacetophenone (3MAP) (100 mM) were added to the salt chamber and 1.56 g amine transaminase (ATA) (6 U/mL) to the biocatalyst chamber. During the reaction the formed product (*S*)-1-(3-methoxyphenyl)ethylamine (3MPEA) can diffuse through the membrane and result in crystal growth with 3DPPA on the product salt seed crystals, while the cells containing the ATA are retained by the membrane. Every 24 h samples were taken from both chambers of the reactor and measured by gas chromatography.

2.7. Triple Vessel Procedure

5.14 mL IPA (100 mM) and 3.57 g HEPES buffer (25 mM) were added to 600 mL water and the pH was adjusted to 7.5. From this solution, 80 mL were added to each of the two chambers of the membrane reactor and the remainder divided between the saturator and the crystallizer. 10.3 g donor salt (≙ 60 mM, if it would be fully dissolved) was then added to the saturator and 1 g product salt was added to the crystallizer (159 mg for saturation and 841 mg as seed crystals) (see Figure 2). By switching on the pumps (2.5 L/h) and stirrers (200 rpm), the partially dissolved salts can be distributed throughout the system, while crystalline salt is retained by the filters in the respective vessels. To start the reaction, 741 mg PLP (5 mM) and 8.24 mL 3MAP (≙ 100 mM) were added to the saturator and 1.56 g ATA (1 U/mL) to the biocatalyst chamber of the membrane reactor. Samples were taken regularly from the biocatalyst chamber of the membrane reactor and measured by gas chromatography, to re-adjust the 3MAP concentration to the initial concentration of 100 mM, based on the observed conversion. As long as solid donor salt is still present in the saturator, it is not necessary to add additional material.

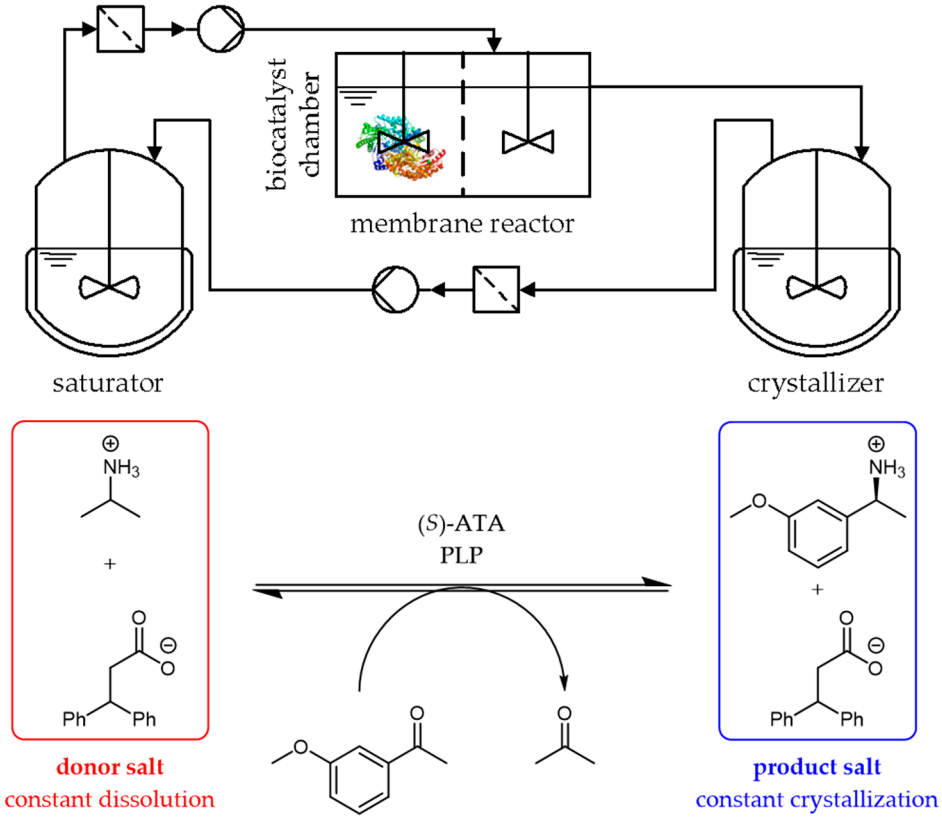

Figure 2. Reaction scheme of the continuous transaminases-catalyzed reaction with in situ donor salt dissolution (left) and product salt crystallization (right) in separated vessels.

2.8. Sampling

Samples of the suspension (500 µL) were taken periodically and 50 µL conc. NaOH was added to completely solve the undissolved salts and quench the reaction. Then 500 µL cyclopentylmethyl ether (CPME) was added to extract substrate and product, mixed by a vortex mixer and then centrifuged (2 min, 3000 rpm) to improve phase separation. From the organic layer, 200 µL was taken and was diluted with 800 µl CPME, combined with 200 µL of a 25 mM n-decane solution in CPME (internal standard) and subsequently analyzed by gas chromatography.

2.9. Chromatography

Concentration was measured with a Trace 1310 gas chromatograph by Thermo Scientific (Dreieich, Germany), equipped with a 1300 flame ionization detector and an Agilent Capillary HP-5 19091 J-433 (0.25 mm × 30 m × 0.25 µm). n-Decane was used as internal standard in all measurements. Temperatures of injector and detector were set to 250 °C. Temperature profile started at 90 °C, followed by a heating rate of 2 K/min to 100 °C, 20 K/min to 130 °C, 2 K/min to 138 °C and 20 K/min to 160 °C.

2.10. X-ray Powder Diffraction (XRPD)

Solid samples were measured via x-ray powder diffraction (XRPD) to discriminate the solid composition of donor salt and/or product salt. Powder x-ray diffraction data were collected on a Stoe Stadi-P with germanium-monochromatised Cu-Kα-radiation (λ = 1.5418 Å) in horizontal transmission/Debey-Scherrer geometry. The x-rays were detected with a position sensitive detector in the 2Theta range from 5 to 35°. The 40 kV high voltage and 40 mA current were generated by a Seifert high voltage generator (ID 3003). The equipment was controlled and the raw data were handled with the software STOE WinXPOW (version 2.25, 2009). The position of the 2Theta and ω-circle were

adjusted with the (111)-reflex of crystalline silicon (2Theta = 28.44°). All samples were measured as flat preparation between two layers of poly acetate foil. The sample was spun around its center during the measurement and the ω-circle was also spun with 1/2 2Theta.

2.11. Nuclear Magnetic Resonance (NMR)

^{1}H NMR and ^{13}C NMR spectra were recorded with a Bruker AVANCE 250 II, AVANCE 300 III and AVANCE 500. Chemical shifts are reported in parts per million relative to the solvent peak as an internal reference. Splitting patterns are indicated as follows: s, singlet; d, doublet; t, triplet; m, multiplet (see Appendix A).

3. Results and Discussion

Initial studies of the integrated use of crystallization in amine transaminase-catalyzed reactions included a direct application of a carboxylic acid, which yields the crystallization of the product amine salt but specifically avoids the crystallization of the donor amine isopropylamine as its salt (donor salt) [16]. This application of this concept results in a moderate apparent shift of the reaction equilibrium towards the product side but is unfortunately often limited to batch reactions and relatively low substrate concentrations due to a continuously increasing amount of solid product salt stopping the entire reaction.

In this study we present an alternative continuous approach towards this reactive crystallization, which intentionally includes the presence of the originally undesired donor amine salt isopropylammonium 3,3-diphenylpropionate. The donor amine salt dissolves continuously and thus release stoichiometric amounts of isopropylammonium and 3,3-diphenylpropionate into solution. Any excess beyond the solubility limit remains as a dispersed solid phase in the reaction mixture. This basically limits the amount of amine in solution to an absolute minimum, in contrast to conventional approaches using high excesses of isopropylamine in solution, which may cause limited enzyme stability [30,31]. Similarly, the substrate 3MAP is continuously dissolved in the solution up to its solubility limit, ensuring a constant 3MAP concentration in the aqueous solution throughout the process. Consequently, the reaction equilibrium in solution is based on the aqueous phase concentration since it is only accessible by the biocatalyst. The conversion towards the products leads to a continuous removal of the educts from the aqueous solution, which is adjusted to the original concentration due to the above mentioned solubility equilibrium. The reaction cycle is closed by the final continuous crystallization of the product amine salt, which removes in stoichiometric amounts the dissolved 3,3-diphenylpropionate anion. The only byproduct is acetone, which evaporates quite easily from solution due to its high vapor pressure at 30 °C [30]. Applications at large scale will require additional solutions to remove acetone effectively from solution to avoid a full stop of the in situ-product crystallization and the inhibition of the biocatalyst, for example, via stripping with an inert gas.

The presence of two solid salt phases requires a separation into two vessels to avoid an undesired mixing. In this work we present a triple vessel system, which separates both solid phases and the catalyst from each other, which enables the above mentioned continuous reaction mode (Figure 2). A membrane reactor is applied to retain the biocatalyst (amine transaminase from *Ruegeria pomeroyi*) behind a polyvinylidene fluoride membrane (PVDF), while the filtered mother liquor is pumped via peristaltic pumps through a crystallizer for product salt crystallization, a saturator for donor salt saturation and eventually back into the membrane reactor to close the loop. An exception is the connection between the membrane reactor and the crystallizer, which is directly fed by an overflow from the higher positioned membrane reactor.

3.1. Salt Solubilities

The solubility difference between both salts, donor salt and product salt, is the main parameter within the shown reaction mode. The donor salt must have a significantly higher solubility than the

product salt, which will only then crystallize selectively from solution. Using the 3,3-diphenylpropionate (3DPPA) as the anion results in a solubility difference of approx. 50 mM between the donor salt (IPA-3DPPA) and the product salt (3MPEA-3DPPA) (Figure 3). For the investigated biocatalytic reaction system the concentration of the donor salt remains for above pH 7 and 30 °C, at >50 mM, while the product salt is considerably less soluble at approx. 5 mM, depending on the chosen pH in solution (Figure 3A). These results are comparable with the model product amine salt 1-phenylethylammonium 3,3-diphenylpropionate in an earlier study [30]. Please note that the shown concentrations may be altered by the presence of other salts such as other buffer components, impurities and especially the additionally used isopropylamine. Changes in temperature will also affect the solubilities of these two main salts, however the observed effect is relatively small. As shown in Figure 3B at pH 7.5 no significant effect is visible and the donor salt remains strongly more soluble than the product amine salt. The choice of temperature is fortunately mostly controlled by the temperature optimum of the biocatalyst itself, which limits the choice of reaction temperature to a narrow range at 30 °C.

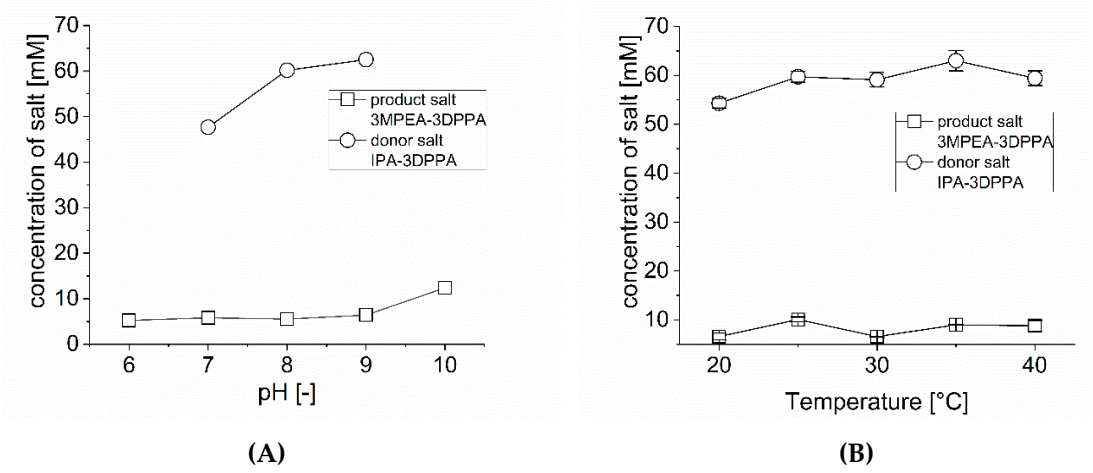

Figure 3. pH- and temperature-dependent solubility profile of the donor salt IPA-3DPPA and product salt 3MPEA-3DPPA; (**A**) pH dependency in 50 mM phosphate buffer at 30 °C; (**B**) temperature dependency in 25 mM HEPES buffer pH 7.5.

3.2. Single Membrane Reactor

The central membrane reactor is the key component within the triple vessel concept. The applied membrane primarily retains the biocatalyst (whole *E. coli* cells) in the biocatalyst chamber from the remaining solution and both solid salts, IPA-3DPPA and 3MPEA-3DPPA, in the salt chamber (Figure 4). During the reaction, IPA-3DPPA is continuously consumed as the amount of product salt increases and eventually accumulates as the only solid phase.

The dissolved reactants diffuse freely between both chambers and a relevant diffusion limitation was not observed (full equilibrium conditions can be achieved within ca. 10 min). This approach provides an alternative to classical encapsulation and immobilization approaches and thus prevents undesired deactivation or diffusion problems of the biocatalytic reaction system [32–36]. The applied PVDF transfer membrane is fully biocompatible and was described by Wachtmeister et al. in 2014 for a lyase-catalyzed reaction [37]. In addition, the use of a membrane reactor offers a simple adjustment of the biocatalytic synthesis system without interfering with the solid salt phases, including the addition or a full exchange of the biocatalyst during the reaction. In addition, the accumulation of inactivated biocatalyst in combination with an undesired mixing with the product salt is prevented, which simplifies downstream processing enormously to a simple filtration step.

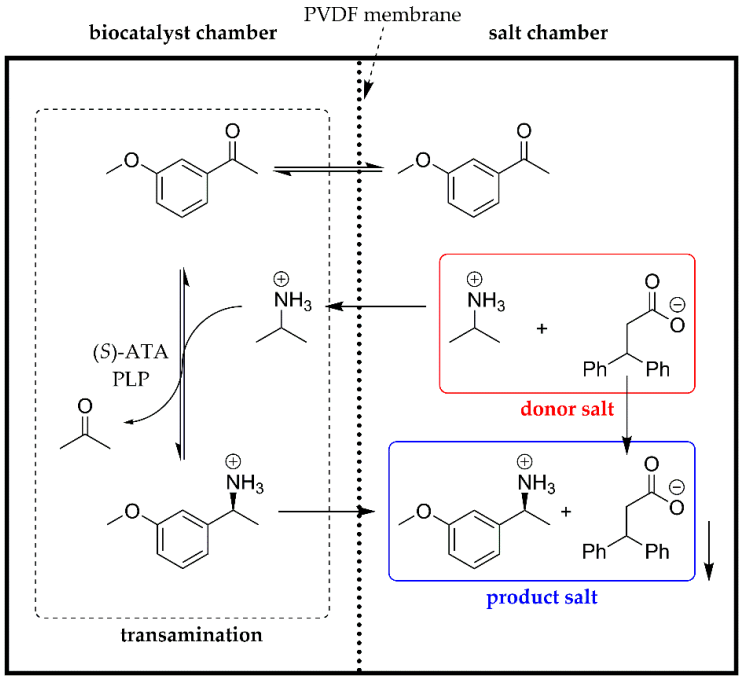

Figure 4. Reaction flow in the membrane reactor.

As shown in Figure 5, a batch experiment of the membrane reactor, without any connection to a saturator and crystallizer, allows the conversion of 55 mM 3MAP to the corresponding product amine salt 3MPEA-3DPPA. The product salt accumulates exclusively in the salt chamber, while the donor salt IPA-3DPPA is consumed in parallel in the salt chamber. A small amount of the product amine is always present in the biocatalyst chamber, which relates to the solubility limit of the product salt in solution. Eventually the reaction stops at approx. 55 mM product concentration due to an accumulation of acetone in the aqueous phase due to the absence of an active acetone removal step, which equals the equilibrium position of this biochemical reaction. Due to absence of an any observable substrate and product inhibition at the chosen reaction conditions, the only rate determining step is the available catalytic activity of the biocatalyst, which leaves a lot of room for optimization. Transport through the membrane and crystal growth are always significantly faster and did not limit the overall process.

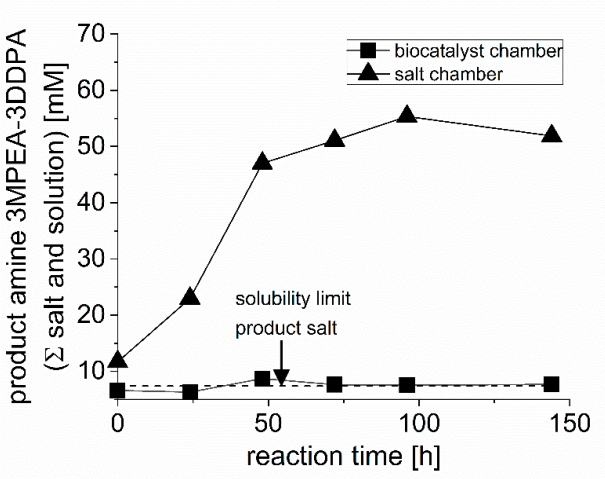

Figure 5. 3MPEA concentration curve in the chambers of the membrane reactor, 30 °C, 25 mM HEPES buffer pH 7.5, 100 mM 3MAP, 100 mM IPA-3DPPA, 100 mM additional isopropylamine and 5 mM PLP (within entire solution).

3.3. Combined Triple Vessel Concept

To permanently separate the salts from each other, the salt chamber of the membrane reactor is replaced by a flow-through chamber connected to two other vessels (see Figure 2). The donor salt is placed in the so-called saturator, which is placed directly before the membrane reactor. Here it can dissolve the donor salt continuously up to the solubility limit to keep the isopropylammonium and 3,3-diphenylpropionate concentrations in solution constant, which is later lowered by the biocatalytic reaction and the product crystallization step. The product salt is formed in the crystallizer, which is positioned after the membrane reactor and facilitates a constant crystal growth due to a slightly oversaturated product salt solution coming from the membrane reactor. Throughout the reaction donor salt is constantly consumed by dissolution in the saturator and equally product salt collected by crystal growth in the crystallizer. In the solution all concentrations are at an almost steady state except the above mentioned small oversaturation of the product salt and small undersaturation of the donor salt directly after the membrane reactor. In contrast to the single membrane reactor, an accumulation of acetone and thus limited equilibrium conversion seems not to be present here due the high surface area of the vessels and probably the applied tubing, which are permeable to acetone. In total, 1 g of biocatalytically produced product amine salt was obtained throughout the reaction. By dissolving the product salt in a basic solution, the product amine can be extracted into cyclopentylmethyl ether (CPME). By adding HCl, the hydrochloride of the product amine can be precipitated and filtered off, which was described in an earlier study [30]. The system remained fully stable over 33 h with a constant process productivity of 1.2 g/(L·d) (Figure 6). After 33 h an undesired product salt crystallization occurred in the biocatalyst chamber, which decreased overall productivity significantly. The crystal morphology between donor salt (platelets) and product salt (needles) is clearly different (Figure 7).

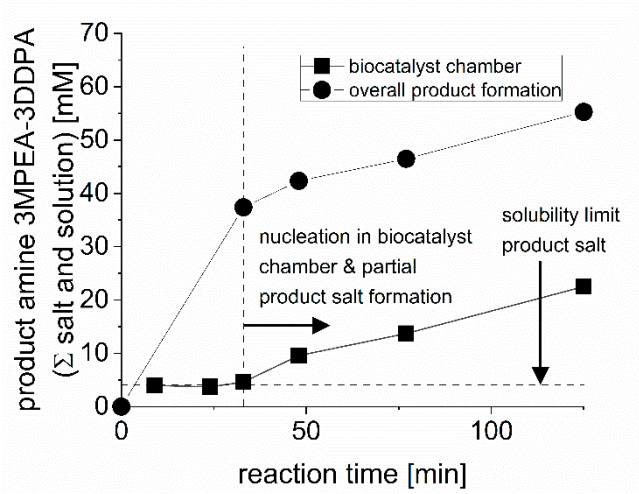

Figure 6. Product formation in the combined triple vessel concept; 30 °C, 25 mM HEPES buffer pH 7.5, 100 mM 3MAP, 60 mM IPA-3DPPA, 100 mM additional isopropylamine and 5 mM PLP (within entire solution).

The product salt was easily obtained from the reaction solution by a simple filtration and a single rinse with distilled water. The solid phase does not contain any cell or protein residue. The purity was determined by NMR with >99.5% and the enantiomeric excess was determined by high-performance liquid chromatography with >99.5%. XRPD analysis also showed that no donor salt formation occurred in the crystallizer and similarly no product salt was found in the saturator (Figure 8).

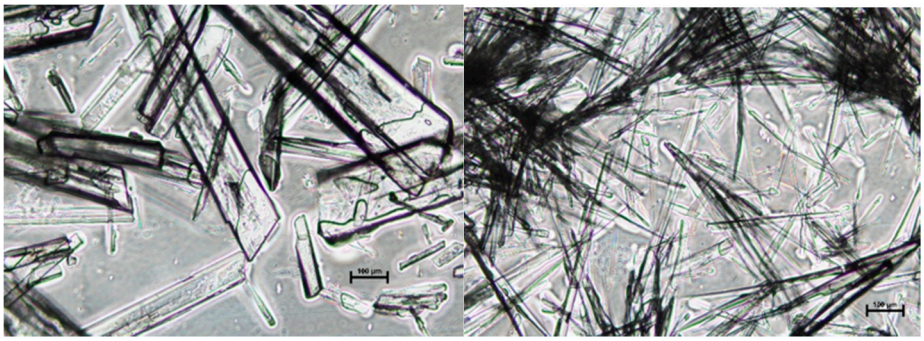

Figure 7. Crystal morphology of donor salt (left) and product salt (right).

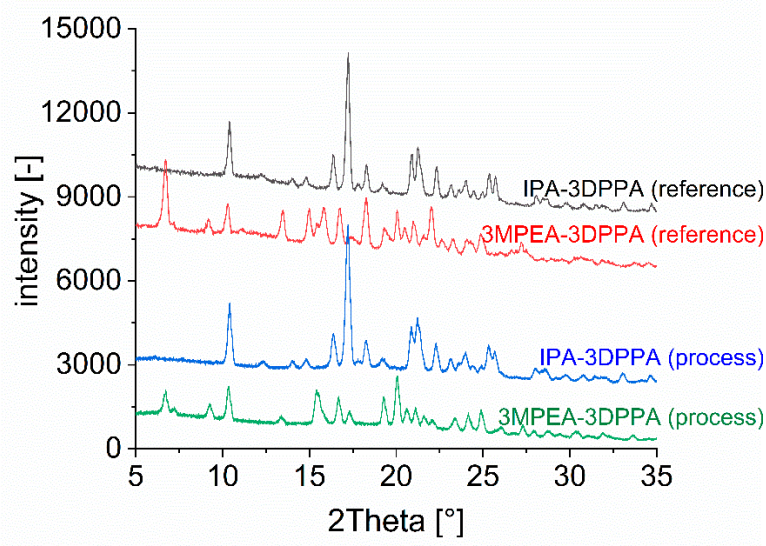

Figure 8. X-ray powder diffraction (XRPD) -analysis of donor and product salt; reference substances and samples from combined triple vessel concept.

4. Summary and Conclusions

In this study we reported the development of a continuously operated amine transaminase-catalyzed reaction, which is based on the integration of a reactive crystallization step for the in situ-removal of the product amine as a product salt. The presented concept involves the use of a membrane reactor, which retains the whole cell biocatalyst and two separate vessels for the application and collection of the donor salt (saturator) and product salt (crystallizer). The saturator provides a constant concentration of the required donor amine salt isopropylammonium 3,3-diphenylpropionate simultaneous to the crystallizer that collects the product amine salt (*S*)-1-(3-methoxyphenyl)ethylammonium 3,3-diphenylpropionate.

In conclusion, the shown triple vessel concept with its central membrane reactor and final crystallizer allows to overcome the very unfavorable chemical reaction equilibrium of the amine transaminase-catalyzed reaction in a continuously operated vessel concept. A fully stoichiometric reaction was achieved, which is not obtained in classical reaction concepts using isopropylamine as donor amine. The spatial separation of biocatalyst, saturator and crystallizer allows a full control of these components, including its separate removal and recycling after usage. The shown concept achieves very high product purity by the integrated crystallization step with only very few downstream-processing steps. The application of the membrane reactor provides a localization of the biocatalyst and prevents the use of potentially harmful immobilization techniques. The herein achieved space-time-yield of 1.2 g/(L·d) is directly correlated with the applied biocatalyst activity, which will increase in parallel with higher biocatalyst loadings. Future studies will also target the optimization of the shown concept in order to improve process productivity in such a continuous reaction mode. This primarily includes

techniques to prevent the undesired nucleation by an optimized reactor design and the use of purified enzyme within the biocatalyst chamber.

Author Contributions: Conceptualization, J.v.L. and D.H.; methodology, D.H., P.K. and E.T.; formal analysis, D.H. and J.v.L.; investigation, D.H. and J.v.L.; writing—original draft preparation, D.H.; writing—review and editing, J.v.L. and E.T.; visualization, D.H. and J.v.L.; supervision, J.v.L.; project administration, J.v.L.; funding acquisition, J.v.L. All authors have read and agreed to the published version of the manuscript.

Funding: Funding by German Research Foundation (DFG, grant LA 4183/1-1), the Central Innovation Program SME of the Federal Ministry for Economic Affairs and Energy (ZIM, grant number 16KN073233) and the Leibniz ScienceCampus Phosphorus Research Rostock (grant CryPhos), is gratefully acknowledged.

Acknowledgments: The authors thank Hubert Bahl and Ralf-Jörg Fischer for their continuous support in microbiology, Dirk Michalik and Heike Borgwaldt for their assistance with NMR measurements, Martin Köckerling and Florian Schröder for their assistance with XRPD-measurements and Sandra Diederich and Rike Thomsen for technical and experimental support. We acknowledge financial support by Deutsche Forschungsgemeinschaft and Universität Rostock within the funding programme Open Access Publishing.

Conflicts of Interest: The authors declare no conflict of interest.

Abbreviation

3DPPA	3,3-Diphenylpropionic acid
3MAP	3′-Methoxyacetophenone
3MPEA	(*S*)-1-(3-Methoxyphenyl)ethylamine
3MPEA-3DPPA	(*S*)-1-(3-Methoxyphenyl)ethylammonium 3,3-diphenylpropionate (product salt)
ATA	Amine transaminase
CPME	Cyclopentylmethyl ether
HEPES	2-[4-(2-Hydroxyethyl)piperazin-1-yl]ethanesulfonic acid
IPA	Isopropylamine
IPA-3DPPA	Isopropylammonium 3,3-diphenylpropionate (donor salt)
NMR	Nuclear magnetic resonance
PLP	Pyridoxal 5′-phosphate
PVDF	Polyvinylidene fluoride transfer membrane
XRPD	X-ray powder diffraction

Appendix A

Appendix A.1. NMR-Data

Appendix A.1.1. Donor Salt IPA-3DPPA

^{1}H-NMR (373.2 K, DMSO-d6, 500.13 MHz, δ in ppm): 7.29–7.09 (m, 10H, Ar H), 4.47 (t, *J* = 7.7 Hz,1H, CH), 3.07 (m, *J* = 6.4 Hz, 1H, CH), 2.86 (d, *J* = 7.7 Hz, 2H, CH_2), 1.05 (d, *J* = 6.4 Hz, 6H, CH_3), NH_3^+ not given

^{13}C-NMR (373.1 K, DMSO-d6, 125.76 MHz, δ in ppm): 172.8 (CO_2), 144.7 (Ar), 127.7 (Ar), 127.2 (Ar), 125.4 (Ar), 46.9 (CH), 41.9 (CH_2), 41.6 (CH), 23.2 (CH_3)

Appendix A.1.2. Product Salt 3MPEA-3DPPA

^{1}H-NMR (373.1 K, DMSO-d6, 500.13 MHz, δ in ppm): 7.32–6.74 (m, 14H, Ar H), 5.16 (s, 3H, NH_3^+), 4.46 (t, *J* = 7.8 Hz, 1H, CH), 4.01 (q, *J* = 6.7 Hz, 1H, CH), 3.76 (s, 3H, O–CH_3), 2.97 (d, *J* = 7.8 Hz, 2H, CH_2), 1.29 (d, *J* = 6.7 Hz, 3H, CH_3)

^{13}C-NMR (373.2 K, DMSO-d6, 125.76 MHz, δ in ppm): 172.0 (CO_2), 159.0 (Ar), 149.2 (Ar), 143.9 (Ar), 128.5 (Ar), 127.8 (Ar), 127.1 (Ar), 125.5 (Ar), 117.7 (Ar), 111.5 (Ar), 111.3 (Ar), 54.6 (O–CH_3), 50.0 (CH), 46.5 (CH), 40.1 (CH2), 24.9 (CH_3)

References

1. Narancic, T.; Davis, R.; Nikodinovic-Runic, J.; O′ Connor, K.E. Recent developments in biocatalysis beyond the laboratory. *Biotechnol. Lett.* **2015**, *37*, 943–954. [CrossRef] [PubMed]
2. Choi, J.-M.; Han, S.-S.; Kim, H.-S. Industrial applications of enzyme biocatalysis: Current status and future aspects. *Biotechnol. Adv.* **2015**, *33*, 1443–1454. [CrossRef] [PubMed]

3. Reetz, M.T. Biocatalysis in organic chemistry and biotechnology: Past, present, and future. *J. Am. Chem. Soc.* **2013**, *135*, 12480–12496. [CrossRef] [PubMed]
4. Munoz Solano, D.; Hoyos, P.; Hernaiz, M.J.; Alcantara, A.R.; Sanchez-Montero, J.M. Industrial biotransformations in the synthesis of building blocks leading to enantiopure drugs. *Bioresour. Technol.* **2012**, *115*, 196–207. [CrossRef]
5. Clouthier, C.M.; Pelletier, J.N. Expanding the organic toolbox: A guide to integrating biocatalysis in synthesis. *Chem. Soc. Rev.* **2012**, *41*, 1585–1605. [CrossRef]
6. Bornscheuer, U.T.; Huisman, G.W.; Kazlauskas, R.J.; Lutz, S.; Moore, J.C.; Robins, K. Engineering the third wave of biocatalysis. *Nature* **2012**, *485*, 185–194. [CrossRef]
7. Wohlgemuth, R. The locks and keys to industrial biotechnology. *New Biotechnol.* **2009**, *25*, 204–213. [CrossRef]
8. Ni, Y.; Holtmann, D.; Hollmann, F. How Green is Biocatalysis? To Calculate is To Know. *ChemCatChem* **2014**, *6*, 930–943. [CrossRef]
9. Hülsewede, D.; Meyer, L.-E.; von Langermann, J. Application of In Situ Product Crystallization and Related Techniques in Biocatalytic Processes. *Chem. Eur. J.* **2019**, *25*, 4871–4884. [CrossRef]
10. Enz, A. Phenylcarbamate for the Inhibition of Acetylcholinesterase. Patent DE3805744C2, 24 February 1988.
11. Farlow, M.R.; Cummings, J.L. Effective pharmacologic management of Alzheimer's disease. *Am. J. Med.* **2007**, *120*, 388–397. [CrossRef]
12. Emre, M. Rivastigmine in Parkinson's Disease Dementia. *CNS Drugs* **2006**, *20*, 748–750. [CrossRef]
13. Fuchs, M.; Koszelewski, D.; Tauber, K.; Kroutil, W.; Faber, K. Chemoenzymatic asymmetric total synthesis of (S)-Rivastigmine using omega-transaminases. *Chem. Commun.* **2010**, *46*, 5500–5502. [CrossRef] [PubMed]
14. Steffen-Munsberg, F.; Vickers, C.; Kohls, H.; Land, H.; Mallin, H.; Nobili, A.; Skalden, L.; van den Bergh, T.; Joosten, H.-J.; Berglund, P.; et al. Bioinformatic analysis of a PLP-dependent enzyme superfamily suitable for biocatalytic applications. *Biotechnol. Adv.* **2015**, *33*, 566–604. [CrossRef] [PubMed]
15. Mallin, H.; Höhne, M.; Bornscheuer, U.T. Immobilization of (R)- and (S)-amine transaminases on chitosan support and their application for amine synthesis using isopropylamine as donor. *J. Biotechnol.* **2014**, *191*, 32–37. [CrossRef]
16. Hülsewede, D.; Tänzler, M.; Süss, P.; Mildner, A.; Menyes, U.; Langermann, J. von. Development of an in situ-Product Crystallization (ISPC)-Concept to Shift the Reaction Equilibria of Selected Amine Transaminase-Catalyzed Reactions. *Eur. J. Org. Chem.* **2018**, *18*, 2130–2133. [CrossRef]
17. Payer, S.E.; Schrittwieser, J.H.; Kroutil, W. Vicinal Diamines as Smart Cosubstrates in the Transaminase-Catalyzed Asymmetric Amination of Ketones. *Eur. J. Org. Chem.* **2017**, *2017*, 2553–2559. [CrossRef]
18. Satyawali, Y.; Ehimen, E.; Cauwenberghs, L.; Maesen, M.; Vandezande, P.; Dejonghe, W. Asymmetric synthesis of chiral amine in organic solvent and in-situ product recovery for process intensification: A case study. *Biochem. Eng. J.* **2017**, *117*, 97–104. [CrossRef]
19. Heintz, S.; Borner, T.; Ringborg, R.H.; Rehn, G.; Grey, C.; Nordblad, M.; Kruhne, U.; Gernaey, K.V.; Adlercreutz, P.; Woodley, J.M. Development of in situ product removal strategies in biocatalysis applying scaled-down unit operations. *Biotechnol. Bioeng.* **2017**, *114*, 600–609. [CrossRef]
20. Rehn, G.; Ayres, B.; Adlercreutz, P.; Grey, C. An improved process for biocatalytic asymmetric amine synthesis by in situ product removal using a supported liquid membrane. *J. Mol. Catal. B Enzym.* **2016**, *123*, 1–7. [CrossRef]
21. Gomm, A.; Lewis, W.; Green, A.P.; O'Reilly, E. A New Generation of Smart Amine Donors for Transaminase-Mediated Biotransformations. *Chem. Eur. J.* **2016**, *22*, 12692–12695. [CrossRef]
22. Börner, T.; Rehn, G.; Grey, C.; Adlercreutz, P. A Process Concept for High-Purity Production of Amines by Transaminase-Catalyzed Asymmetric Synthesis: Combining Enzyme Cascade and Membrane-Assisted ISPR. *Org. Process Res. Dev.* **2015**, *19*, 793–799. [CrossRef]
23. Green, A.P.; Turner, N.J.; O'Reilly, E. Chiral amine synthesis using omega-transaminases: An amine donor that displaces equilibria and enables high-throughput screening. *Angew. Chem. Int. Ed.* **2014**, *53*, 10714–10717. [CrossRef] [PubMed]
24. Cassimjee, K.E.; Branneby, C.; Abedi, V.; Wells, A.; Berglund, P. Transaminations with isopropyl amine: Equilibrium displacement with yeast alcohol dehydrogenase coupled to in situ cofactor regeneration. *Chem. Commun.* **2010**, *46*, 5569–5571. [CrossRef] [PubMed]

25. Rehn, G.; Adlercreutz, P.; Grey, C. Supported liquid membrane as a novel tool for driving the equilibrium of omega-transaminase catalyzed asymmetric synthesis. *J. Biotechnol.* **2014**, *179*, 50–55. [CrossRef] [PubMed]
26. Höhne, M.; Bornscheuer, U.T. Biocatalytic Routes to Optically Active Amines. *ChemCatChem* **2009**, *1*, 42–51. [CrossRef]
27. Simon, R.C.; Richter, N.; Busto, E.; Kroutil, W. Recent Developments of Cascade Reactions Involving ω-Transaminases. *ACS Catal.* **2014**, *4*, 129–143. [CrossRef]
28. Koszelewski, D.; Lavandera, I.; Clay, D.; Rozzell, D.; Kroutil, W. Asymmetric Synthesis of Optically Pure Pharmacologically Relevant Amines Employing ω-Transaminases. *Adv. Synth. Catal.* **2008**, *350*, 2761–2766. [CrossRef]
29. Slabu, I.; Galman, J.L.; Lloyd, R.C.; Turner, N.J. Discovery, Engineering, and Synthetic Application of Transaminase Biocatalysts. *ACS Catal.* **2017**, *7*, 8263–8284. [CrossRef]
30. Hülsewede, D.; Dohm, J.-N.; von Langermann, J. Donor Amine Salt-Based Continuous in situ- Product Crystallization in Amine Transaminase-Catalyzed Reactions. *Adv. Synth. Catal.* **2019**, *361*, 2727–2733. [CrossRef]
31. Meng, Q.; Capra, N.; Palacio, C.M.; Lanfranchi, E.; Otzen, M.; van Schie, L.Z.; Rozeboom, H.J.; Thunnissen, A.-M.W.H.; Wijma, H.J.; Janssen, D.B. Robust ω-Transaminases by Computational Stabilization of the Subunit Interface. *ACS Catal.* **2020**, 2915–2928. [CrossRef]
32. Grabner, B.; Nazario, M.A.; Gundersen, M.T.; Loïs, S.; Fantini, S.; Bartsch, S.; Woodley, J.M.; Gruber-Woelfler, H. Room-temperature solid phase ionic liquid (RTSPIL) coated ω-transaminases: Development and application in organic solvents. *Mol. Catal.* **2018**, *452*, 11–19. [CrossRef]
33. Miložič, N.; Lubej, M.; Lakner, M.; Žnidaršič-Plazl, P.; Plazl, I. Theoretical and experimental study of enzyme kinetics in a microreactor system with surface-immobilized biocatalyst. *Chem. Eng. J.* **2017**, *313*, 374–381. [CrossRef]
34. Rehn, G.; Grey, C.; Branneby, C.; Lindberg, L.; Adlercreutz, P. Activity and stability of different immobilized preparations of recombinant E. coli cells containing ω-transaminase. *Process Biochem.* **2012**, *47*, 1129–1134. [CrossRef]
35. Sheldon, R.A. Enzyme Immobilization: The Quest for Optimum Performance. *Adv. Synth. Catal.* **2007**, *349*, 1289–1307. [CrossRef]
36. Uthoff, F.; Sato, H.; Gröger, H. Formal Enantioselective Hydroamination of Non-Activated Alkenes: Transformation of Styrenes into Enantiomerically Pure 1-Phenylethylamines in Chemoenzymatic One-Pot Synthesis. *ChemCatChem* **2017**, *9*, 555–558. [CrossRef]
37. Wachtmeister, J.; Jakoblinnert, A.; Kulig, J.; Offermann, H.; Rother, D. Whole-Cell Teabag Catalysis for the Modularisation of Synthetic Enzyme Cascades in Micro-Aqueous Systems. *ChemCatChem* **2014**, *6*, 1051–1058. [CrossRef]

© 2020 by the authors. Licensee MDPI, Basel, Switzerland. This article is an open access article distributed under the terms and conditions of the Creative Commons Attribution (CC BY) license (http://creativecommons.org/licenses/by/4.0/).